International Journal of Mass Spectrometry 289 (2010) 6–10

Contents lists available at ScienceDirect

International Journal of Mass Spectrometry

journal homepage: www.elsevier.com/locate/ijms

Uncertainty assessment of Si molar mass measurements

G. Mana[a,*], E. Massa[a], S. Valkiers[b], G.-D. Willenberg[c]

[a] INRIM - Istituto Nazionale di Ricerca Metrologica, Str. delle Cacce 91, 10135 Torino, Italy
[b] IRMM - Institute for Reference Materials and Measurements, Retieseweg 11, 2440 Geel, Belgium
[c] PTB - Physikalisch-Technische Bundesanstalt, Bundesallee 100, 38116 Braunschweig, Germany

ARTICLE INFO

Article history:
Received 27 July 2009
Received in revised form 2 September 2009
Accepted 3 September 2009
Available online 11 September 2009

PACS:
82.80.Ms
07.75.+h
06.20.–f
06.20.Dk

MSC:
62P35
92E99

Keywords:
Isotope ratio mass spectrometry
Si molar mass
Metrology
Measurement uncertainty

ABSTRACT

The uncertainty of the Si molar mass measurement is theoretically investigated by means of a two-isotope model, with particular emphasis to the role of this measurement in the determination of the Avogadro constant. This model allows an explicit calibration formula to be given and propagation of error analysis to be made. It also shows that calibration cannot correct for non-linearity.

1. Introduction

The Avogadro constant, $N_A = 6.02214179(30) \times 10^{23}\,\mathrm{mol}^{-1}$ [1,2], is the molar number of entities. It expresses the ^{12}C mass in kilograms according to $m(^{12}\mathrm{C}) = M(^{12}\mathrm{C})/N_A$, where $M(^{12}\mathrm{C}) = 12\,\mathrm{g\,mol}^{-1}$ is the molar mass, and connects the atomic and macroscopic scales. A method to derive it from the density ρ, the molar mass M, and the unit cell volume V_0 of a crystal – namely, in all experiments, silicon – was suggested by Bragg in 1913 [3]; it relies on $N_A = nM/(\rho V_0)$, where n is the number of atom per unit cell. Since the comparisons between the official copies and the international prototype of the kilogram show a divergence with time as large as 5×10^{-8} kg since their first calibration in 1889, to determine N_A to an accuracy allowing the kilogram definition to be based on the ^{12}C mass [4–6], the relative uncertainty of the silicon molar mass measurement must be reduced to at least $2 \times 10^{-8} M(\mathrm{Si})$. With this in view, several metrology institutes are participating in an international research project (International Avogadro Coordination, IAC) for the determination of N_A using a highly enriched ^{28}Si crystal. Isotope enrichment and crystal production were completed and a 5 kg crystal with ^{28}Si enrichment higher than 99.99% is now available for measurements [7].

The isotope amount ratios are measured by gas mass spectrometry; the measured quantities being ion-current ratios [8–12]. Only in the ideal case can the measured ratios be identified with the isotope amount ratios; in practice, conversion factors are required, which are close to unity and are obtained by measuring synthesized amount ratios embodied in mixtures of enriched Si isotopes.

By application of concepts suggested by De Bièvre's [13] and Friedrich [14], we have investigated the uncertainty of the molar mass measurement with the aid of a two-isotope model and *Mathematica* [15]. This model allows an explicit calibration formula to be obtained. In addition, we examine how the molar mass of highly enriched ^{28}Si could be obtained, in a way similar to isotope dilution, simultaneously to calibration. The measurement accuracy depends on the ion-current uncertainty and on how the ion currents relate to the isotope amount fractions. An important result is the demon-

---

* Corresponding author. Tel.: +39 011 3919728; fax: +39 011 3919926.
E-mail addresses: g.mana@inrim.it (G. Mana), e.mssa@inrim.it (E. Massa), Staf.Valkiers@ec.europa.eu (S. Valkiers), Gerd-Dietmar.Willenberg@ptb.de (G.-D. Willenberg).

1387-3806/$ – see front matter © 2009 Elsevier B.V. All rights reserved.
doi:10.1016/j.ijms.2009.09.005

stration that by calibration it is impossible to correct offsets in the ion-current measurements. A strict proportionality between the isotope amount fractions and the ion currents is essential to calibration, whatever the composition of the mixture used might be.

2. Two-isotope model

For the sake of simplicity, let us consider silicon as composed by two isotopes only, namely, ^{28}Si and ^{29}Si. Hence, the molar mass is

$$M = \frac{M_{28} + RM_{29}}{1+R}, \tag{1}$$

where M_{28} and M_{29} are the molar masses of ^{28}Si and ^{29}Si and $R = x/(1-x)$ is the ratio between the isotope amount fractions $x_{29} = x$ and $x_{28} = 1 - x$ of ^{29}Si and ^{28}Si. By leaving off the M_{28} and M_{29} uncertainties, which are irrelevant, the relative uncertainty of the molar mass is

$$\frac{u_M}{M} = Cx(1-x)\frac{u_R}{R}, \tag{2}$$

where u_R is the R uncertainty and the C coefficient accounts for effective mass difference between the Si isotopes. To examine to the extend to which this approximation supplies useful information, let us re-evaluate (2) in the actual three-isotope case. Therefore,

$$M = \frac{M_{28} + R_{29}M_{29} + R_{30}M_{30}}{1 + R_{29} + R_{30}}, \tag{3}$$

where the symbols have their usual meaning. Provided the R_{29} and R_{30} uncertainties are equal, at least approximately, the relative uncertainty of the molar mass is still given by (2), where $R = R_{29} + R_{30}$,

$$C \approx \frac{\Delta M\sqrt{(1-R_{30})^2 + (2+R_{29})^2}}{M}, \tag{4}$$

and $\Delta M \approx 1$ g/mol. The C coefficient ranges from 0.08 (when $R_{29} \approx R_{30} \approx 0$) to 0.11 (when $R_{29} \approx R_{30} \approx 1$); in the following, since we are mostly interested in the natural silicon and enriched ^{28}Si, we will use $C = 0.08$.

The isotope amount ratio is related to the measured $r = I_{29}/I_{28}$ ratio between the ion currents by $R = \kappa_0 r$, where κ_0 is a calibration factor. Consequently,

$$\frac{u_R}{R} = \sqrt{\left(\frac{u_{\kappa_0}}{\kappa_0}\right)^2 + \left(\frac{u_r}{r}\right)^2}, \tag{5}$$

where u_{κ_0} and u_r are the calibration and current-ratio uncertainties.

To complete the analysis of the propagation of uncertainty, we need a model to relate the ion currents and isotope amount fractions. The basic model is given in [16]; in the present paper, a proportional relationship is assumed. To compensate for source noise and drift, measurements are performed by using a single Faraday cup in peak jumping mode. The jumping mode and the subsequent data analysis, a demodulation of the data with respect to the peak indexing, remove any linear drift. In this way a set of current ratios is obtained, where the dividend and divisor are as simultaneous as possible. The sample in the expansion vessel changes isotopic composition because of the isotope fractionation process in the molecular gas flow from the inlet system to the ion source. Extrapolation of the current ratios to the start time of the measurement via a non-linear least-squares regression is thus required. Let the extrapolated values of the ion currents be proportional to the isotope amount fractions, that is,

$$I_n = a_n x_n I_T, \tag{6}$$

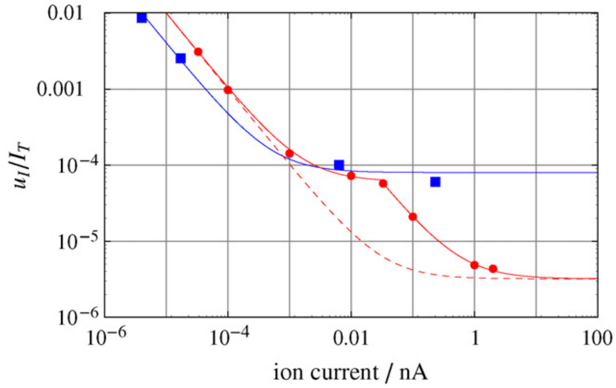

Fig. 1. Uncertainty of the ion-current. Squares (blue) indicate the ion-current noise, bullets (red) the calibration uncertainty of the ammeter electronics. Different feedback resistors are used for currents below and above 0.03 nA; typically, 400 G Ω and 3 G Ω, respectively. This explains the discontinuous character of the calibration uncertainty. The u_1 and u_2 parameters for the solid (blue) and dashed (red) lines are given in Table 1 (cases a and b), $I_T = 1$ nA. (For interpretation of the references to color in this figure legend, the reader is referred to the web version of the article.)

where $n = 28$ and 29, a_n accounts for fractionation, and $I_T = I_{28} + I_{29} \approx 1$ nA is the total ion-current, and let

$$u_n = (u_1 + u_2 x_n)I_T \tag{7}$$

be the equivalent current uncertainty after ratio extrapolation.

The $u_{1,2}$ contributions were investigated experimentally. In a first test, performed by the IRMM, the ion-current noise was considered; the ratios – expected to be one by definition – obtained from typical sequences (100 data, with 8 s integration time) of the same current were extrapolated to the time zero and the equivalent current uncertainties were estimated backward. In a second test, performed by the Physikalish-Technische Bundesanstalt, it was investigated the calibration uncertainty of the detection electronics, a feedback ammeter with a transimpedance amplifier which converts the input current into a voltage [17]. Results are shown in Fig. 1. In the low current regime, the limiting factor is the ammeter calibration; in the high current one, it is the ion-source noise. It must be noted that this analysis does not consider the residual contributions of systematic effects after they have been identified and corrected for—for instance, background signal, cross talk between ion currents, non-linearity. These uncertainty contributions must be included in the u_1 term and will be further discussed in Section 4.

The relative uncertainty of the current-ratio is

$$\frac{u_r}{r} = \sqrt{\left[\frac{u_1 + u_2(1-x)}{1-x}\right]^2 + \left[\frac{u_1 + u_2 x}{x}\right]^2}, \tag{8}$$

which is shown in Fig. 2; the parameter values used are listed in Table 1. By putting (2), (5) and (8) together, the relative uncertainty

Table 1
Detection limit, u_1, and ion-source, u_2, contributions to the ion-current uncertainty used in numerical examples. Values are expressed in relative units, with respect to the total ion-current, see Eq. (6).

Case	u_1	u_2
a	4×10^{-8}	0.8×10^{-4}
b	1×10^{-7}	3.2×10^{-6}
c	8×10^{-7}	2.0×10^{-4}
d	2×10^{-7}	1.0×10^{-4}

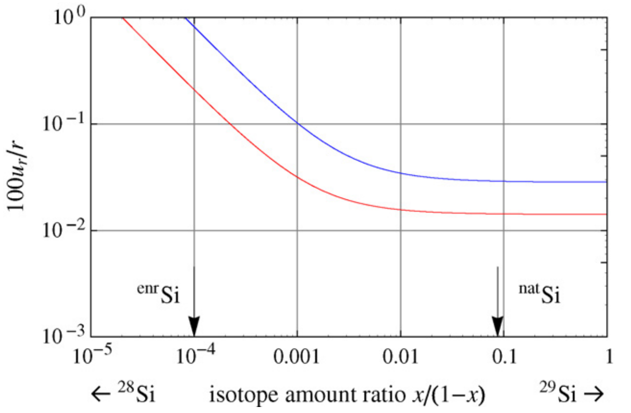

Fig. 2. Uncertainty of the ion-current ratio. The u_1 and u_2 parameters for the upper (blue) and lower (red) lines are given in Table 1 (cases c and d). Since r and $1/r$ share the same relative uncertainty, the plot is symmetric with respect to the $x/(1-x) = 1$ axis. (For interpretation of the references to color in this figure legend, the reader is referred to the web version of the article.)

of the molar mass is

$$\frac{u_M}{M} = 0.08x(1-x)\sqrt{\left(\frac{u_{\kappa_0}}{\kappa_0}\right)^2 + \left[\frac{u_1 + u_2(1-x)}{1-x}\right]^2 + \left[\frac{u_1 + u_2 x}{x}\right]^2}, \tag{9}$$

where no implicit dependence on x remains. Fig. 3 (black line) evidences that, owing to the $x(1-x)$ factor, the higher the enrichment, the smaller the calibration contribution u_{κ_0}/κ_0 to the molar mass uncertainty. However, as shown by (8), u_r/r is inversely proportional to the same factor; therefore, systematic effects and current detection-limit (summarized by the u_1 contribution to the current uncertainty) set a bound to the uncertainty (dashed lines). Since the calibration uncertainty is independent of the sample isotopic composition,

$$\lim_{x\to 0} \frac{u_M}{M} = 0.08u_1, \tag{10}$$

which is the basic equation to anticipate the uncertainty of molar mass measurements of enriched ^{28}Si. As shown in Fig. 2, u_r/r is minimum when $R = 1$, but, in (2), this minimum values is amplified by the $x(1-x)$ term; the trade-off result depends on the ion-current uncertainty model.

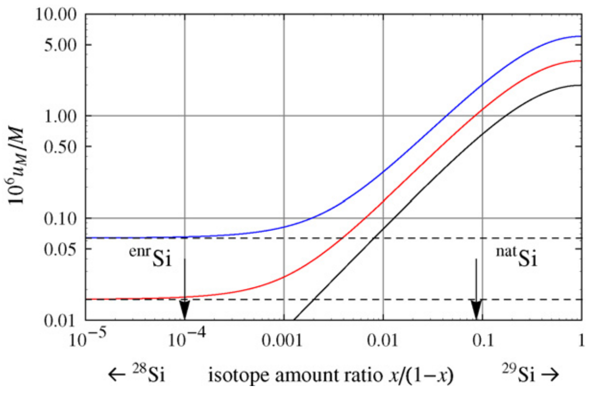

Fig. 3. Molar-mass uncertainty. The u_1 and u_2 parameters for the upper (blue) and lower (red) lines are given in Table 1 (cases c and d), $u_{\kappa_0}/\kappa_0 = 10^{-4}$. Dashed lines are the $0.08u_1$ limits when $x \to 0$. Since R and $1/R$ share the same relative uncertainty, the plot is symmetric with respect the $x/(1-x) = 1$ axis; the black line is the $0.08x(1-x)u_{\kappa_0}/\kappa_0$ limit uncertainty when $u_1 = u_2 = 0$. (For interpretation of the references to color in this figure legend, the reader is referred to the web version of the article.)

3. Calibration

Calibration is similar to the isotope dilution technique and consists in blending a Si sample with a spike, a weighed amount of Si having a different isotopic composition, and in measuring the isotope amount ratios in sample, spike, and mixture. Let us indicate the parent materials by A and B and the synthetic mixture by S; that is, with a misuse of language, n_A A+ n_B B $\rightarrow$ n_S S. If the mass fractions of the sample and the spike are $1 - w$ and w, their amount fractions are $1 - \alpha$ and

$$\alpha = \frac{n_B}{n_S} = \frac{w/M_B}{(1-w)/M_A + w/M_B}, \tag{11}$$

where M_A and M_B are the sample and spike molar masses. Consequently, the fraction of ^{29}Si in the mixture is

$$x_S = (1-\alpha)x_A + \alpha x_B. \tag{12}$$

The calibration factor is found by solving

$$\kappa_0 r_A = \frac{x_A}{1-x_A}, \tag{13a}$$

$$\kappa_0 r_B = \frac{x_B}{1-x_B}, \tag{13b}$$

$$\kappa_0 r_S = \frac{(1-\alpha)x_A + \alpha x_B}{1-(1-\alpha)x_A - \alpha x_B} \tag{13c}$$

By elimination of x_A and x_B from (13c) and remembering (11) and $M_{A,B} = (1 - x_{A,B})M_{28} + x_{A,B}M_{29}$, we obtain

$$\kappa_0 = \frac{M_{28}}{M_{29}} \frac{w(r_A - r_B) + r_S - r_A}{w(r_B - r_A)r_S + (r_A - r_S)r_B}. \tag{14}$$

In the limit when $x_A \to 0$ and $x_B \to 1$ (or vice versa), this formula simplifies to $\kappa_0 \approx R_S/r_S$, which is the basis of recursive determinations of the calibration factor.

The calibration uncertainty is calculated by observing that the κ_0 variance is $u^2_{\kappa_0} = \mathbf{J}^T\mathbf{CJ}$, where $\mathbf{J}$ is the Jacobian of $\kappa_0(r_A, r_B, r_S)$,

$$\mathbf{C} = \begin{bmatrix} u_r^2(x_A) & 0 & 0 \\ 0 & u_r^2(x_B) & 0 \\ 0 & 0 & u_r^2(x_S) \end{bmatrix}, \tag{15}$$

and $u^2_r(x)$ is given by (8). As expected from $\kappa_0 \approx R_S/r_S$, Fig. 4 shows that u_{κ_0}/κ_0 is always greater than u_{r_S}/r_S, the excess arising from the R_S uncertainty. When x_S approaches x_A or x_B, u_{κ_0} diverges; in these cases, the calibration equations are no longer independent. These limits correspond to $\alpha = 0$ and $\alpha = 1$, where r_S replicates (13a) or (13b) and κ_0 is indeterminate. When x_S, which is in the

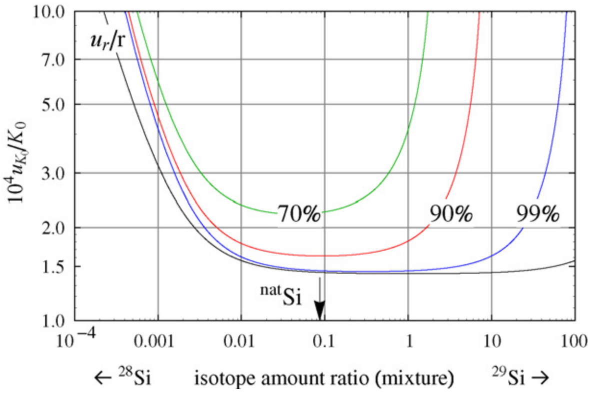

Fig. 4. Ion-current contribution to calibration uncertainty. The u_1 and u_2 parameters are given in Table 1 (entry d) and $x_A = 0.008\%$; blue, red, and green lines correspond to $x_B = 99\%$, 90%, and 70%. The black line is the uncertainty of the ion-current ratio. (For interpretation of the references to color in this figure legend, the reader is referred to the web version of the article.)

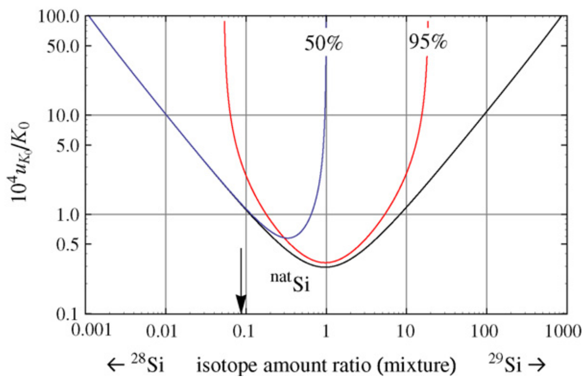

Fig. 5. Weighing contribution to the calibration uncertainty. The balance resolution is 10 μg, the mixture mass is 1 g. The red line corresponds to both the parent materials enriched up to 95%, the blue one to $x_A = 0\%$ and $x_B = 50\%$. The black line is the limit uncertainty when both the parent materials are pure isotopes. (For interpretation of the references to color in this figure legend, the reader is referred to the web version of the article.)

$x_A < x_S < x_B$ range, is midway between x_A and x_B, the calibration uncertainty approaches u_{r_S}/r_S. With highly enriched parent materials, the minimum uncertainty,

$$\frac{u_{\kappa_0}}{\kappa_0} \approx \lim_{x_S \to 0.5} \frac{u_{r_S}}{r_S} = 2\sqrt{2}\left(\frac{u_1 + u_2}{2}\right), \tag{16}$$

is achieved when $x_S = 0.5$, that is, when the mixture is a 1:1 blend.

The weighing contribution to u_{κ_0} is shown in Fig. 5. The propagation-of-uncertainty analysis has been carried out on the basis of (14), by taking account that

$$w = \frac{m_{29}}{(m_{28} + m_{29})} \tag{17}$$

and

$$u_w = \sqrt{1 + 2w(w-1)}\,\frac{u_m}{m_T}, \tag{18}$$

where m_n is the ^{n}Si mass in the mixture, $m_T = m_{28} + m_{29} = 1$ g is the total mass, and $u_m = 10\,\mu$g is the balance resolution. Figs. 4 and 5 indicate that the optimal blend is a 1:1 mixture.

The sample molar mass, as well those of the spike and mixture, can be obtained simultaneously to calibration. In fact, by using (14) in (13a),

$$R_A = \frac{M_{28}}{M_{29}} \frac{[w(r_A - r_B) + r_S - r_A]r_A}{w(r_B - r_A)r_S + (r_A - r_S)r_B} \tag{19}$$

is obtained and similar equations hold for R_B and R_S. This equation is significant for the determination of molar mass by isotope dilution; the relevant uncertainty analysis is shown in Fig. 6. The figure evidences also that, in order to approach the lower bound of the measurement uncertainty, it is essential to calibrate the mass spectrometer with a mixture of highly enriched Si isotopes.

4. Calibration non-linearity

The previous analysis assumes perfect proportionality between the ion currents and isotope amount fractions, but, when absolute molar mass measurements are carried out at the $10^{-8}M$ uncertainty level, any phenomenon modifying this proportionality makes $R = \kappa(x)r$ non-linear because the calibration factor depends on the to isotopic composition. An important case study is when

$$I_n = (a_n x_n + b_n)I_T = a_n(x_n + c_n)I_T, \tag{20}$$

where the b_n symbol, with $n = 28$ and 29, has an obvious meaning and c_n is the corresponding, apparent or actual, variation of the isotope fraction. This model describes contamination by natural silicon, isobar currents, zero offsets of the ammeter electronics, current leakages, and background currents not fully eliminated or compensated. Though the ion currents are still linear functions of x_n, the calibration factor,

$$\kappa(x) = \frac{\kappa_0 x(1 - x + c_{28})}{(1 - x)(x + c_{29})}, \tag{21}$$

depends now on the isotopic composition. By comparing (20) with (6) and (7), we see that, in order to neglect non-linearities, c_n must not exceed 2×10^{-7}. Therefore, it would be very useful to identify non-linearities by calibration.

The basic idea, given a sample T with a^{29}Si fraction equal to x_T, is to estimate $\kappa(x_T)$ by calibration with a mixture having the same^{29}Si fraction. In (13a)–(13c), $\kappa(x)$ should be evaluated for different x values, namely, x_A, x_B, and x_S, but, instead, a constant value is used. What is the value of κ_0 when it is calculated according to (14)? If $x_S = x_T$, is $\kappa_0 \approx \kappa(x_T)$? To answer these questions we must write (14) in terms of the ion currents and, in turn, in terms of x_A and x_B by means of (6), (11), and (12). If the ion currents are proportional to x_n as expressed by (6), we obtain the trivial identity $\kappa_0 = a_{28}/a_{29}$, as expected.

Contrary, if we use (20) for (6), we obtain

$$\kappa \approx \kappa_0 - 0.035(c_{28} + c_{29}), \tag{22}$$

where $c_n = b_n/I_T$ and only the first order correction has been retained. Therefore, the calculated calibration factor is still independent of the mixture composition and depends very weakly on the current offsets. In particular, it is different from $\kappa(x_T)$ and this naive way to correct for the b_n term in (20) fails.

To understand why, let us first consider the contamination by natural Si. Since to calibrate the spectrometer according to (14) it is not necessary to know the isotopic compositions of the parent materials A and B, nor κ_0 depends on them, it does not matter if these materials get contaminated. Obviously, the molar masses obtained by application of (19) and (1) are those of the contaminated materials, but, as long as we are interested in κ_0 only, this is not significant. Next, we observe that, as mathematically expressed by (6), any offset is equivalent to a contamination, to the extent that the observation of the offset alone is not sufficient to discriminate among its origins. However, in the case of a current offset, the mixture composition (12) does not change consistently with the above apparent changes of the parent-material compositions. This explains the residual small correction to κ_0 in (22).

The calibration and molar mass errors, $|\Delta\kappa/\kappa_0| = |\kappa_0(x)/\kappa_0 - 1|$ and $|\Delta M/M| = 0.08x(1-x)|\Delta\kappa/\kappa_0|$, are shown in Figs. 7 and 8; if the isotope amount ratio is $x/(1-x) = c_{29}/c_{28}$ then $\kappa(x) = \kappa_0$ no

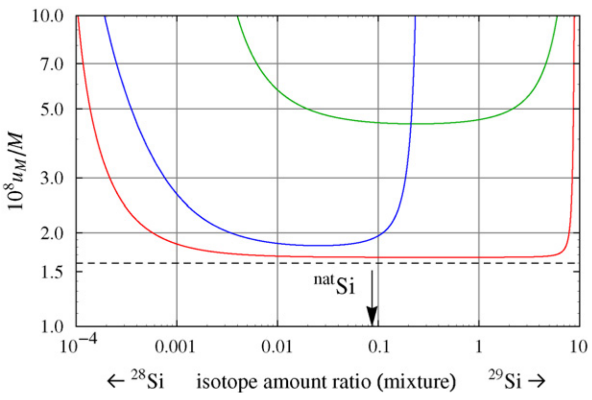

Fig. 6. Uncertainty of molar mass measurements. Weighing uncertainty has been neglected and the u_1 and u_2 parameters are given in Table 1 (entry d). The red and blue lines correspond to $x_A = 0.008\%$ and $x_B = 90\%$ and 20%, respectively; the green line corresponds to $x_A = 0.2\%$ and $x_B = 90\%$. The dashed line is the $0.08u_1$ lower bound. (For interpretation of the references to color in this figure legend, the reader is referred to the web version of the article.)

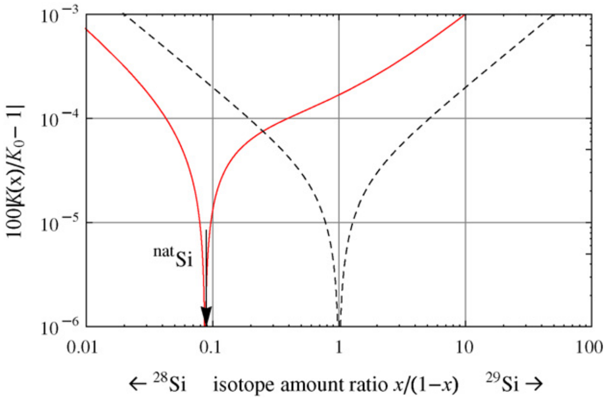

Fig. 7. Calibration error. Solid (red) line is 1 part per million contamination by ^{nat}Si ($c_{28} = 8 \times 10^{-8}$ and $c_{29} = 92 \times 10^{-8}$), dashed (black) line is background ($c_{28} = c_{29} = 2 \times 10^{-7}$). (For interpretation of the references to color in this figure legend, the reader is referred to the web version of the article.)

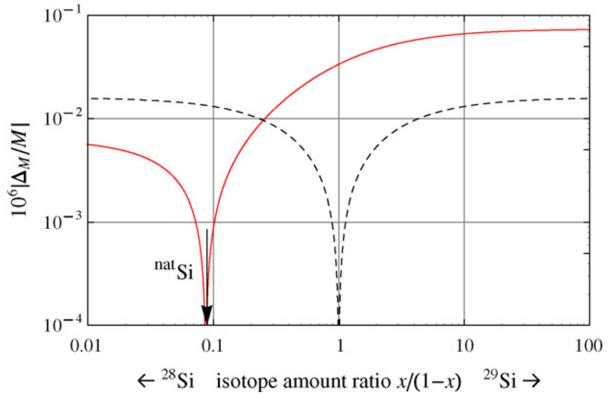

Fig. 8. Molar mass error. Solid (red) line is 1 part per million contamination by ^{nat}Si ($c_{28} = 8 \times 10^{-8}$ and $c_{29} = 92 \times 10^{-8}$), dashed (black) line is background ($c_{28} = c_{29} = 2 \times 10^{-7}$). (For interpretation of the references to color in this figure legend, the reader is referred to the web version of the article.)

error occurs. The reason is that the c_{29}/c_{28} value is the isotope amount ratio of the equivalent contamination and, if the material to be measured has the same composition, obviously, no contamination actually occurs. For instance, if $c_{28} = c_{29}$ the isotope amount ratio of the equivalent contamination is one, as shown in Figs. 7 and 8.

5. Conclusions

When testing theoretical concepts and technical capabilities, correct uncertainty assignments – neither too small nor too large – are essentials. The present analysis supplies a mathematical background for the assessment of the contribution of the Si molar mass measurement to the uncertainty of the N_A determination. This analysis is also a tool for optimal design of measurements and calibration. Results suggest that good calibration requires mixtures approaching the 1:1 ratio of the relevant isotopes and that, provided enough material is available to make negligible the weighing errors, the calibration uncertainty is limited only by the uncertainty of the ion-current measurement.

Since silicon is not a mono-isotopic element, the molar mass of ^{28}Si (the most abundant isotope) requires correction for the minority isotopes; the higher the enrichment is, the smaller the correction will be and, consequently, the uncertainty. However, the detection limit of current measurements and systematic effects fix a lower bound to the uncertainty, no matter what the enrichment could be. Ion currents have a central role; in order to achieve the targeted $2 \times 10^{-8}M$ uncertainty, their measurement uncertainty must be reduced to $2 \times 10^{-7}I_T$, where I_T is the total ion-current. Additionally, the uncertainty model of the ion currents and the model parameters must be carefully investigated and put through experimental tests. Future investigations also aim at extending results to the actual case of three isotopes.

Acknowledgments

This work received funds from the European Community's Seventh Framework Programme ERA-NET Plus – grant 217257, from the Regione Piemonte – grant D64, and from the Compagnia di San Paolo.

References

[1] A.D. McNaught, A. Wilkinson, Compendium of Chemical Terminology, 2nd ed., Blackwell Science, Oxford, 1997.

[2] P.J. Mohr, B.N. Taylor, D.B. Newel, Rev. Mod. Phys. 80 (2008) 633–730.

[3] W.H. Bragg, W.L. Bragg, Proc. R. Soc. A 88 (1913) 428–438.

[4] P. Becker, P. De Bièvre, K. Fujii, M. Glaeser, B. Inglis, H. Luebbig, G. Mana, Metrologia 44 (2007) 1–14.

[5] P. Becker, Metrologia 40 (2003) 366–375.

[6] G. Mana, G. Zosi, Riv. Nuovo Cimento 18 (1995) 1–23.

[7] P. Becker, D. Schiel, H.-J. Pohl, A.K. Kaliteevski, O.N. Godisov, M.F. Churbanov, G.G. Devyatykh, A.V. Gusev, A.D. Bulanov, S.A. Adamchik, V.A. Gavva, I.D. Kovalev, N.V. Abrosimov, B. Hallmann-Seiffert, H. Riemann, S. Valkiers, P. Taylor, P. De Bièvre, E.M. Dianov, Meas. Sci. Technol. 17 (2006) 1854–1860.

[8] P. De Bièvre, Metrologia 32 (1995) 103–110.

[9] S. Valkiers, Y. Aregbe, P. De Bièvre, Int. J. Mass Spectrom. Ion Proc. 173 (1998) 55–63.

[10] S. Valkiers, h. Kipphardt, T. Ding, K.C. Mayer, P. Taylor, Int. J. Mass Spectrom. Ion Proc. 193 (1999) 1–8.

[11] K. Ruße, S. Valkiers, P. Taylor, Int. J. Mass Spectrom. Ion Proc. 235 (2004) 255–262.

[12] R. Kessel, A Novel Approach to Uncertainty Evaluation of Complex Measurements in Isotope Chemistry, Ph.D. Thesis, University of Antwerp, 2003.

[13] P.J. De Bièvre, G.H. Debus, Nucl. Instrum. Methods 32 (1965) 224–228.

[14] P. Becker, H. Friedrich, K. Fujii, W. Giardini, G. Mana, A. Picard, H.-J. Pohl, H. Riemann, S. Valkiers, Meas. Sci. Technol. 20 (2009) 092002.

[15] Wolfram Reasearch, Inc., Mathematica Version 6.0.3.0, Wolfram Reasearch, Inc., Champaign, IL, 2008.

[16] M. Varlam, S. Valkiers, M. Berglund, P. Taylor, R. Gonfiantini, P. de Bièvre, Int. J. Mass Spectrom. 269 (2008) 78–84.

[17] G.D. Willenberg, PTB Measurement Report, Physikalisch-Technische Bundesanstalt, Braunschweig, 2008.